



Attitude tracking control of a quadrotor UAV subject to external disturbance with L_2 performance

Tianpeng Huang · Tieshan Li 

Received: 7 June 2022 / Accepted: 1 March 2023 / Published online: 20 March 2023
© The Author(s), under exclusive licence to Springer Nature B.V. 2023

Abstract Attitude stability plays an important role in the safe flight of quadrotor unmanned aerial vehicle (UAV). This paper aims to address the problem of attitude control of quadrotor UAV. The mathematical model of quadrotor system subject to external disturbance is first introduced. Then, a finite-time disturbance observer (FTDO) is developed to effectively compensate for external disturbance. It is proved that the disturbance observation error can be guaranteed to converge to zero in finite time. Based on the designed FTDO, a backstepping sliding mode control technique is proposed to stabilize three attitude angles of a quadrotor UAV, which can eliminate the tracking errors of attitude channel to zero asymptotically. Moreover, by constructing an auxiliary equation, the bound of transient attitude tracking error in terms of L_2 norm is derived. Finally, the comparative simulations are carried out to illustrate the effectiveness of the proposed control scheme and several statistical indexes are given to quantitatively evaluate the performance in terms of observation error, tracking error and control signal.

Keywords Quadrotor UAV · Backstepping sliding mode control · Finite-time disturbance observer · L_2 norm bound

1 Introduction

In recent years, the quadrotor UAV has attracted the attention of many researchers, thanks to its simple operation procedure and some unique advantages, such as vertical take-off and landing, hovering, etc. Stable flight is one of the most concerned issues in quadrotor systems. To achieve this goal, research on the controller design of quadrotor drones has been done.

Currently, many control methods have been applied to the design of attitude controller of quadrotor, such as proportional-integral-derivative control [1], active disturbance rejection control [2], H_∞ synthesis technique [3], model predictive control [4], model reference adaptive control [5] and linear quadratic control [6]. Among these control techniques, SMC is a well-known control technique that is widely utilized to construct the robust controller for nonlinear system. In [7–9], an integral SM was adopted to design attitude controller for a quadrotor. In [10–12], several adaptive SMC strategies have been considered to stabilize attitude channels of a quadrotor system. In [13–15], a terminal SMC was presented to design robust flight control system for a quadrotor. However, there is a problem of singularity in terminal SMC. Therefore, a nonsingular terminal SMC was proposed to address this prob-

T. Huang · T. Li (✉)
School of Automation Engineering, University of Electronic Science and Technology of China, Xiyuan Avenue, Chengdu 611731, Sichuan, China
e-mail: tieshanli@126.com

T. Huang
e-mail: tphuang@uestc.edu.cn

lem [16, 17]. In addition, backstepping control is also a widely used control approach based on recursive design idea, which has been introduced to design quadrotor controller. In [18–21], a backstepping approach was applied to the attitude dynamics of a quadrotor. Then, the attitude trajectory tracking is achieved. However, the problem of explosion of complexity exists in the backstepping. To overcome this issue, command filter [22–24], tracking differentiator [25], optimization technique [26] were applied to the backstepping control, respectively. In [27, 28], two adaptive backstepping methods were introduced to design attitude controller of a quadrotor. Furthermore, to fully combine the advantages of SMC and backstepping control, some researches focus on backstepping sliding mode control (BSSMC) of quadrotor UAV. In [29–31], a BSSMC was developed to accomplish the attitude stabilization for a quadrotor. In [32, 33], a backstepping control combined with nonsingular terminal SMC was employed to construct an attitude controller for a quadrotor UAV.

When a quadrotor system flies outdoors, it will always encounter external disturbance, such as wind. Therefore, it is necessary to consider the suppression of disturbance in controller design. In [12, 30], the stabilization of quadrotor system was guaranteed by selecting that the controller gain was greater than the upper bound of disturbance. In [17, 33], by designing an adaptive law for the upper bound of disturbance in the developed controller, the disturbance could be suppressed. As a result, the stability of the closed-loop system could be achieved. Such an idea of disturbance rejection does not require the prior information of disturbance, but the adaptive algorithm may cause parameter drift of the estimated state. Moreover, designing disturbance observer is an effective method to compensate for disturbance in the design of controller. In [10, 13, 16, 19, 20, 24, 25, 28, 29, 31, 32, 34, 35], the disturbance observer designed have been integrated into quadrotor controller to eliminate disturbance, where an same assumption that disturbance changes slowly was given in [19, 28, 32]. This means the compensation of disturbance with rapid change may not be realized in [19, 28, 32]. Meanwhile, the estimation error of disturbance was only asymptotically convergent in [10, 24, 29, 34, 35]. Although the finite-time convergence of the estimation error of disturbance was guaranteed in [13, 16], the convergence time was not provided. In [20, 25, 31], an extended state observer was employed to estimate disturbance, which stabilized the

disturbance observation error within a bounded range in finite time. Moreover, some intelligent techniques, such as neural network [36], fuzzy logic system [37] and reinforcement learning [37], combined with the classical algorithms have been applied to the estimation of disturbance.

It is worth noting that the aforementioned works have considered the convergence analysis of steady-state tracking error, but the transient performance of tracking error is not fully considered. To further highlight the gap identified in the literature, a comparative table, i.e. Table 1, is given, where Item A denotes method of disturbance rejection; Item B denotes prior information of disturbance; Item C denotes convergence of disturbance observation error; Item D denotes steady-state performance of tracking error; Item E denotes transient performance of tracking error; Item F denotes evaluation index.

In this paper, to eliminate the adverse effects of external disturbance acting on quadrotor systems, a BSSMC technique based on disturbance observer with finite-time convergence is proposed and then the three attitude angles of the quadrotor drone is stabilized. Moreover, the L_2 performance of the transient tracking error is guaranteed. Therefore, the proposed method has the potential to be extended to other fields to realize practical applications, such as robots and unmanned vehicles. The main contributions of this paper are as follows:

- (i) Compared with the existing DO with asymptotical convergence in [10, 24, 28, 29, 34, 35] and the FTDO without convergence time in [13, 16, 20, 25, 31], in this paper, the proposed FTDO not only guarantees the disturbance observation error converge to zero in finite time, but also gives an explicit reaching time.
- (ii) Unlike the works [29, 31, 32] that only focus the steady-state performance of the tracking error using BSSMC based on DO, the transient performance in term of L_2 norm and the steady-state performance of the tracking error are considered simultaneously in this paper.
- (iii) Compared with [8, 9, 11, 15, 18–26, 29, 30, 32, 36], several statistical indexes are used to quantitatively evaluate the performance of the proposed method in terms of control signal, observation error and tracking error in the comparative simulations.

Table 1 The comparison of disturbance rejection and tracking performance in literature

Reference	Item A	Item B	Item C	Item D	Item E	Item F
[12,30]	Large control gain	Required	Not involved	Considered	Not considered	[12]—Not Used; [30]—Used
[17,33]	Adaptive control	Not required	Not involved	Considered	Not considered	Not Used
[19,28,32]	[19,32]—DO; [28]—Estimator	Required	[19,32]—Asymptotic; [28]—Not proved	Considered	Not considered	[19,28]—Not used; [32]—Used
[10,24,29,34,35]	DO	Not required	Asymptotic	Considered	Not considered	[10,24,34,35]—Not used; [29]—Used
[13,16]	DO	Not required	Finite-time	Considered	Not considered	Not used
[20,25,31]	DO	Not required	Asymptotic	Considered	Not considered	Not used
[36–38]	Intelligent method	Not required	Not involved	Considered	Not considered	[36]—Used; [37,38]—Not used
Our method	DO	Required	Finite-time	Considered	Considered	Used

The remainder of this paper is organized as follows. The dynamics description of the quadrotor is given in Sect. 2. Section 3 recalls some preliminary lemmas. Section 4 introduces the design of the proposed controller based on finite-time disturbance observer and stability analysis. In Sect. 5, the simulation results are presented. Finally, the main conclusions of the paper are presented in Sect. 6.

2 Problem formulation

The sketch of the quadrotor UAV is shown in Fig. 1, where $\{O_e : X_e - Y_e - Z_e\}$ and $\{O_b : X_b - Y_b - Z_b\}$ represent the earth and body frames, respectively. Let $[x \ y \ z]$ denotes the position output of the quadrotor and $[\phi \ \theta \ \varphi]$ represents attitude output of the quadrotor, where ϕ is the roll angle, defined as the angle between the projection of the axis $O_b Z_b$ of the body frame system on the $O_e - Z_e - X_e$ plane of the earth frame system and the axis $O_e Z_e$; θ is the pitch angle, defined as the angle between the projection of the axis $O_b Y_b$ of the body frame system on the $O_e - Y_e - Z_e$ plane of the earth frame system and the axis $O_e Y_e$; φ is the yaw angle, defined as the angle between the projection of the axis $O_b X_b$ of the body frame system on the $O_e - X_e - Y_e$ plane of the earth frame system and the axis $O_e X_e$. In order to maintain the balance of the body, the diagonal rotors (e.g. Rotors 1 and 4) of the quadrotor drone

rotate in the same direction, while the adjacent rotors (e.g. Rotors 2 and 3) rotate in the opposite direction.

In the following, the derivation process of the attitude dynamic model of the quadrotor system will be introduced in detail.

Let $[\bar{p} \ \bar{q} \ \bar{r}]$ represent angular velocity of quadrotor in the coordinate system B . The angular motion dynamics of the quadrotor are [27]

$$\begin{aligned}
 M_x &= I_x \dot{\bar{p}} + (I_z - I_y) \bar{q} \bar{r}, \\
 M_y &= I_y \dot{\bar{q}} + (I_x - I_z) \bar{p} \bar{r}, \\
 M_z &= I_z \dot{\bar{r}} + (I_y - I_x) \bar{p} \bar{q},
 \end{aligned}
 \tag{1}$$

where M_x, M_y, M_z are the components of the resultant torque acting on quadrotor in the three directions of x, y, z , respectively, and I_x, I_y, I_z are the moments of inertia of the quadrotor around x, y, z , respectively.

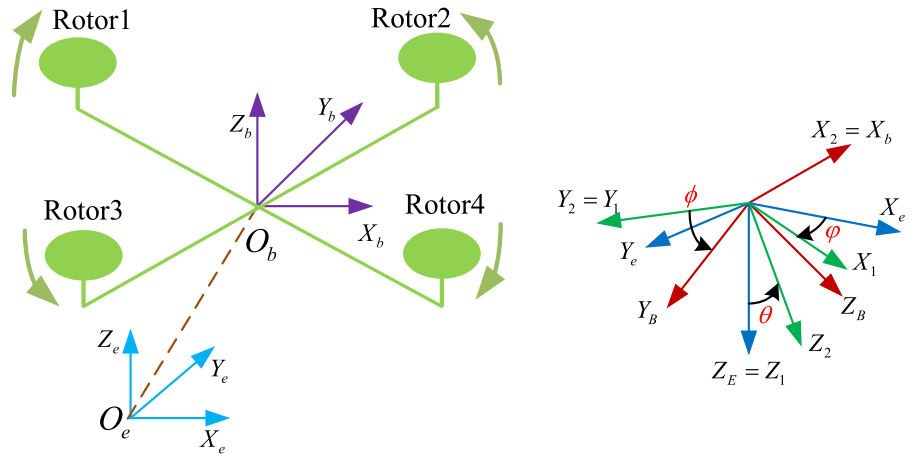
Let M_{lx}, M_{ly}, M_{lz} denote the components of the lifting torque of the quadrotor in the three directions of x, y, z , respectively, which can be expressed as [27]

$$\begin{aligned}
 M_{lx} &= L F_\phi, \\
 M_{ly} &= L F_\theta, \\
 M_{lz} &= f F_\varphi,
 \end{aligned}
 \tag{2}$$

where L is the distance from the center of the rotor to the center of the quadrotor, f is the scaling factor from force to moment and F_ϕ, F_θ , and F_φ are control inputs of attitude channel.

Moreover, the quadrotor is subject to gyroscopic torque during flight, whose components M_{gx}, M_{gy}, M_{gz}

Fig. 1 Quadrotor UAV



around the x , y , and z axes, respectively, are given by [27]

$$\begin{aligned} M_{gx} &= I_r \bar{q} \Omega, \\ M_{gy} &= -I_r \bar{p} \Omega, \\ M_{gz} &= 0. \end{aligned} \tag{3}$$

In (3), I_r is the inertia of each propeller and Ω is the algebraic sum of the four rotors.

Considering (1)–(3), the angular dynamics of the quadrotor can be rewritten in the following form.

$$\begin{aligned} I_x \dot{\bar{p}} &= (I_y - I_z) \bar{q} \bar{r} - I_r \bar{q} \Omega + L F_\phi, \\ I_y \dot{\bar{q}} &= (I_z - I_x) \bar{p} \bar{r} + I_r \bar{p} \Omega + L F_\theta, \\ I_z \dot{\bar{r}} &= (I_x - I_y) \bar{p} \bar{q} + f F_\psi. \end{aligned} \tag{4}$$

Notice that the angular velocity $[\bar{p} \ \bar{q} \ \bar{r}]$ in the coordinate system $\{O_b : X_b - Y_b - Z_b\}$ can be converted to the angular velocity $[\dot{\phi} \ \dot{\theta} \ \dot{\psi}]$ in the coordinate system $\{O_e : X_e - Y_e - Z_e\}$ by [9]

$$\begin{bmatrix} \dot{\phi} \\ \dot{\theta} \\ \dot{\psi} \end{bmatrix} = \begin{bmatrix} 1 & \sin \phi \tan \theta & \cos \phi \tan \theta \\ 0 & \cos \phi & -\sin \phi \\ 0 & \frac{\sin \phi}{\cos \theta} & \frac{\cos \phi}{\cos \theta} \end{bmatrix} \begin{bmatrix} \bar{p} \\ \bar{q} \\ \bar{r} \end{bmatrix}. \tag{5}$$

To ensure flight safety, the attitude angles of the quadrotor are always kept small on purpose during the flight. Thus, it follows from (5) that $[\dot{\phi} \ \dot{\theta} \ \dot{\psi}]^T \approx [\bar{p} \ \bar{q} \ \bar{r}]^T$. In consequence, the attitude dynamics of the quadrotor subjected to external disturbance can be derived from (4),

$$\begin{aligned} \ddot{\phi} &= \frac{(I_y - I_z) \dot{\theta} \dot{\phi} - I_r \dot{\theta} \Omega + L F_\phi}{I_x} + d_\phi, \\ \ddot{\theta} &= \frac{(I_z - I_x) \dot{\phi} \dot{\theta} + I_r \dot{\phi} \Omega + L F_\theta}{I_y} + d_\theta, \\ \ddot{\psi} &= \frac{(I_x - I_y) \dot{\phi} \dot{\theta} + f F_\psi}{I_z} + d_\psi, \end{aligned} \tag{6}$$

where d_ϕ, d_θ, d_ψ are the external disturbances acting on the three attitudes of the quadrotor system in the form of acceleration, respectively. Note that the moment of inertia of the rotor is much smaller than that of the UAV, so the terms $\frac{I_r \dot{\theta} \Omega}{I_x}$ and $\frac{I_r \dot{\phi} \Omega}{I_y}$ can be ignored in the controller design [15]. As a result, (6) can be further derived as

$$\begin{aligned} \ddot{\phi} &= \frac{(I_y - I_z) \dot{\theta} \dot{\phi} + L F_\phi}{I_x} + d_\phi, \\ \ddot{\theta} &= \frac{(I_z - I_x) \dot{\phi} \dot{\theta} + L F_\theta}{I_y} + d_\theta, \\ \ddot{\psi} &= \frac{(I_x - I_y) \dot{\phi} \dot{\theta} + f F_\psi}{I_z} + d_\psi. \end{aligned} \tag{7}$$

3 Preliminaries

Lemma 1 For the following system

$$\dot{\zeta} = f(\zeta), \quad t \geq 0, \quad \zeta(0) = \zeta_0, \tag{8}$$

suppose that there exists a continuous, positive definite function $V(\zeta)$ such that $\dot{V}(\zeta) \leq -\beta V^\alpha(\zeta)$ with positive scalars $\alpha \in (0, 1)$ and $\beta > 0$. Then, the solution of system (8) will converge to zero in finite time $T \leq \frac{1}{\beta(1-\alpha)} V^{1-\alpha}(\zeta_0)$ with $V(\zeta_0)$ being the initial value of $V(\zeta)$ [39].

Lemma 2 Let $V(\zeta)$ be a non-negative scalar function of time on $[0, \infty)$, which satisfies the differential inequality $\dot{V}(\zeta) \leq -\gamma V(\zeta)$, where γ is a positive constant. Then $V(\zeta) \leq e^{-\gamma t} V(\zeta_0), \forall t \in [0, \infty)$, where e is the base of the natural logarithm and $V(\zeta_0)$ is the initial value of $V(\zeta)$ [40].

Lemma 3 *The Rayleigh quotient of symmetric matrix $A \in \mathbb{R}^{n \times n}$ is defined as $R_A = \frac{X^T A X}{X^T X}$ with $X \in \mathbb{R}^n$ and $X \neq 0$. Then we have $\lambda_{\min}(A) \leq R_A \leq \lambda_{\max}(A)$, i.e., $\lambda_{\min}(A)X^T X \leq X^T A X \leq \lambda_{\max}(A)X^T X$, where $\lambda_{\min}(\cdot)$ and $\lambda_{\max}(\cdot)$ are the minimum eigenvalue and maximum eigenvalue of A , respectively [41].*

Lemma 4 *Suppose that: (i) the function $f_1(\tau)$ is monotone on the interval $[a, \infty)$ and $\lim_{\tau \rightarrow \infty} f_1(\tau) = 0$, and (ii) the function $f_2(\tau)$ is integrable on $[a, b]$ for all $b > a$, and the integral function $F_2(\tau) = \int_a^\infty f_2(\tau) d\tau$ is bounded on $[a, \infty)$, then the improper integral $\int_a^\infty f_1(\tau) f_2(\tau) d\tau$ is convergent [42].*

4 Controller design and stability analysis

The control objective is to design an attitude controller to guarantee that the tracking errors of the attitude angles ϕ, θ and φ in (7) can be stabilized in the presence of external disturbance and to guarantee that the L_2 performance of the tracking error is achieved.

Assumption 1 It is assumed that the derivatives of the disturbances d_ϕ, d_θ and d_φ in (7) are uniformly bounded, and satisfy $|\dot{d}_\phi| \leq \delta_\phi, |\dot{d}_\theta| \leq \delta_\theta$ and $|\dot{d}_\varphi| \leq \delta_\varphi$ with known positive constants $\delta_\phi, \delta_\theta, \delta_\varphi$.

Remark 1 Assumption 1 is reasonable, since there is no disturbance that changes infinitely fast in the real world. Moreover, to ensure that the derivative of Lyapunov function is negative, the boundedness of derivative of disturbance needs to be guaranteed.

Remark 2 It can be seen from the dynamic model (7) of the quadrotor that the disturbance acts on the quadrotor system in the form of acceleration. Therefore, the bound of derivative of disturbance could be obtained approximately by measuring the additional acceleration on quadrotor system.

4.1 Controller design

In this section, the design of FTDO and attitude controller will be given, respectively. The FTDO will be first introduce. Let $\tilde{h}_\chi = \dot{\chi}$, where $\chi = \phi, \theta, \varphi$. Define observation error as

$$\begin{aligned} e_{\chi 1} &= \tilde{h}_\chi - \hat{\tilde{h}}_\chi, \\ e_{\chi 2} &= d_\chi - \hat{d}_\chi, \end{aligned} \tag{9}$$

where $\hat{\tilde{h}}_\chi$ and \hat{d}_χ are the estimates of \tilde{h}_χ and d_χ , respectively. The FTDO of attitude channel of the quadrotor is designed as

$$\begin{aligned} \dot{\hat{\tilde{h}}}_\chi &= W_\chi F_\chi + Y_\chi + \xi_1 |e_{\chi 1}|^{\frac{1}{2}} \text{sign}(e_{\chi 1}) + \xi_2 (e_{\chi 1}) + \hat{d}_\chi \\ \dot{\hat{d}}_\chi &= \xi_3 \text{sign}(e_{\chi 1}) + \xi_4 (e_{\chi 1}), \end{aligned} \tag{10}$$

where $\xi = l, p, q$ are the observer parameter to be designed; $\xi = l, W_\chi = \frac{L}{I_x}, Y_\chi = \frac{I_y - I_z}{I_x} \dot{\theta} \dot{\phi}$ when $\chi = \phi$; $\xi = p, W_\chi = \frac{L}{I_y}, Y_\chi = \frac{I_z - I_x}{I_y} \dot{\phi} \dot{\theta}$ when $\chi = \theta$; $\xi = q, W_\chi = \frac{f}{I_z}, Y_\chi = \frac{I_x - I_y}{I_z} \dot{\phi} \dot{\theta}$ when $\chi = \varphi$; $\text{sign}(\cdot)$ denotes signum function. Then the error dynamics of the observer can be obtained by (7), (9) and (10)

$$\begin{aligned} \dot{e}_{\chi 1} &= -\xi_1 |e_{\chi 1}|^{\frac{1}{2}} \text{sign}(e_{\chi 1}) - \xi_2 (e_{\chi 1}) + e_{\chi 2}, \\ \dot{e}_{\chi 2} &= -\xi_3 \text{sign}(e_{\chi 1}) - \xi_4 (e_{\chi 1}) + \dot{d}_\chi. \end{aligned} \tag{11}$$

Then, the design of attitude controller is introduced. Define tracking error as

$$E_\chi = \chi_d - \chi, \tag{12}$$

where χ_d is desired attitude. Furthermore, define

$$\tilde{E}_\chi = -\dot{\chi} + \kappa_\chi, \tag{13}$$

where κ_χ is defined as

$$\kappa_\chi = c_\chi E_\chi + \dot{\chi}_d, \tag{14}$$

with c_χ as a positive constant. Therefore, the time derivative of E_χ can be obtained

$$\begin{aligned} \dot{E}_\chi &= \dot{\chi}_d - \dot{\chi}, \\ &= \dot{\chi}_d + \tilde{E}_\chi - c_\chi E_\chi - \dot{\chi}_d \\ &= -c_\chi E_\chi + \tilde{E}_\chi. \end{aligned} \tag{15}$$

The sliding surface is designed as

$$s_\chi = n_\chi E_\chi + \tilde{E}_\chi, \tag{16}$$

whose derivative with respect to time is

$$\begin{aligned} \dot{s}_\chi &= n_\chi \dot{E}_\chi + \dot{\tilde{E}}_\chi \\ &= n_\chi (-c_\chi E_\chi + \tilde{E}_\chi) + \dot{\kappa}_\chi - \ddot{\chi}, \end{aligned} \tag{17}$$

where n_χ is a positive constant. The attitude controller is designed as

$$\begin{aligned} F_\chi &= \frac{1}{W_\chi} (n_\chi (-c_\chi E_\chi + \tilde{E}_\chi) + \dot{\kappa}_\chi - Y_\chi - \hat{d}_\chi \\ &\quad + E_\chi + h_\chi s_\chi), \end{aligned} \tag{18}$$

where h_χ is a positive constant.

4.2 Stability analysis

Theorem 1 Consider the attitude dynamic model of the quadrotor UAV in (7), if the attitude control law is designed as (18) with the FTDO (10), then we can conclude:

- (i) the observation error (9) of disturbance will be guaranteed to converge to zero in finite time.
- (ii) the attitude output tracking error (12) of the closed-loop system has a global asymptotic stability property;
- (iii) the bound of the transient attitude tracking error in terms of L_2 norm (denoted by $\|\cdot\|_2$) satisfies

$$\|E_X\|_2 \leq \sqrt{\Xi_{X1} + \Xi_{X2} + \Xi_{X3} + \Xi_{X4}}, \tag{19}$$

where

$$\Xi_{X1} = \frac{2 + 2(n_X + c_X)^2 \lambda_X (n_X + c_X)}{\lambda_X + \lambda_X (n_X + c_X)^2} \chi_d^2(0), \tag{20}$$

$$\Xi_{X2} = \frac{2}{\lambda_X + \lambda_X (n_X + c_X)^2} (\dot{\chi}_d(0))^2, \tag{21}$$

$$\Xi_{X3} = \frac{4(n_X + c_X)}{\lambda_X + \lambda_X (n_X + c_X)^2} \chi_d(0) \dot{\chi}_d(0), \tag{22}$$

$$\Xi_{X4} = \frac{-2\lambda_X M_E}{\lambda_X + \lambda_X (n_X + c_X)^2}. \tag{23}$$

Proof Define the following Lyapunov function candidate

$$\bar{V}_X = \frac{1}{2} E_X^2 + \frac{1}{2} s_X^2. \tag{24}$$

The time derivative of \bar{V}_X is

$$\dot{\bar{V}}_X = E_X \dot{E}_X + s_X \dot{s}_X. \tag{25}$$

Applying (15) and (17) to (25) yields

$$\begin{aligned} \dot{\bar{V}}_X &= E_X (-c_X E_X + \tilde{E}_X) \\ &\quad + s_X (n_X (-c_X E_X + \tilde{E}_X) + \dot{\kappa}_X - \ddot{\chi}). \end{aligned} \tag{26}$$

Substituting attitude dynamics (7) of the quadrotor into (26), we have

$$\begin{aligned} \dot{\bar{V}}_X &= E_X (-c_X E_X + \tilde{E}_X) + s_X (n_X (-c_X E_X + \tilde{E}_X) \\ &\quad + \dot{\kappa}_X - W_X F_X - Y_X + d_X). \end{aligned} \tag{27}$$

Substituting the designed attitude controller (18) into (27), we obtain

$$\dot{\bar{V}}_X = -c_X E_X^2 + E_X \tilde{E}_X + s_X (-E_X - h_X s_X + \hat{d}_X - d_X). \tag{28}$$

According to (9), $e_{X2} = -(\hat{d}_X - d_X)$. In the following, we will discuss the convergence of the observation error of the disturbance. Define the following Lyapunov function candidate

$$\begin{aligned} V_X &= 2\xi_3 |e_{X1}| + \xi_4 e_{X1}^2 + \frac{1}{2} e_{X2}^2 + \frac{1}{2} (\xi_1 |e_{X1}|^{\frac{1}{2}} \text{sign}(e_{X1})) \\ &\quad + \xi_2 e_{X1} - e_{X2} \end{aligned} \tag{29}$$

V_X is everywhere continuous and differentiable everywhere except on the subspace $\{(e_{X1}, e_{X2}) \in \mathbb{R}^2 | e_{X1} = 0\}$. The derivative of V_X with respect to time is

$$\begin{aligned} \dot{V}_X &= 2\xi_3 \frac{e_{X1}}{|e_{X1}|} \dot{e}_{X1} + 2\xi_4 e_{X1} \dot{e}_{X1} + e_{X2} \dot{e}_{X2} \\ &\quad + \left(\frac{1}{2} \xi_1^2 \text{sign}(e_{X1}) \dot{e}_{X1} + \xi_1 \xi_2 |e_{X1}|^{\frac{1}{2}} \text{sign}(e_{X1}) \dot{e}_{X1} \right. \\ &\quad \left. - \xi_1 |e_{X1}|^{\frac{1}{2}} \text{sign}(e_{X1}) \dot{e}_{X2} + \frac{1}{2} \xi_1 \xi_2 |e_{X1}|^{-\frac{1}{2}} e_{X1} \dot{e}_{X1} \right) \\ &\quad + \xi_2^2 e_{X1} \dot{e}_{X1} - \xi_2 e_{X1} \dot{e}_{X2} - \frac{1}{2} \xi_1 |e_{X1}|^{-\frac{1}{2}} \dot{e}_{X1} e_{X2} \\ &\quad \left. - \xi_2 \dot{e}_{X1} e_{X2} + e_{X2} \dot{e}_{X2} \right). \end{aligned} \tag{30}$$

Since $\text{sign}(e_{X1}) = \frac{e_{X1}}{|e_{X1}|}$, (30) can be rewritten as

$$\begin{aligned} \dot{V}_X &= \left(2\xi_3 + \frac{\xi_1^2}{2} \right) \frac{e_{X1}}{|e_{X1}|} \dot{e}_{X1} + (2\xi_4 + \xi_2^2) e_{X1} \dot{e}_{X1} \\ &\quad + \frac{3}{2} \xi_1 \xi_2 \frac{e_{X1} \dot{e}_{X1}}{|e_{X1}|^{\frac{1}{2}}} - \xi_2 (\dot{e}_{X1} e_{X2} + e_{X1} \dot{e}_{X2}) \\ &\quad - \xi_1 \left(\frac{1}{2} \frac{\dot{e}_{X1} e_{X2}}{|e_{X1}|^{\frac{1}{2}}} + \frac{e_{X1}}{|e_{X1}|^{\frac{1}{2}}} \dot{e}_{X2} \right) \\ &\quad + 2e_{X2} \dot{e}_{X2}. \end{aligned} \tag{31}$$

Substituting \dot{e}_{X1} and \dot{e}_{X2} in (11) to (31) yields

$$\begin{aligned} \dot{V}_X &= - \left(2\xi_1 \xi_3 + \frac{1}{2} \xi_1^3 \right) |e_{X1}|^{\frac{1}{2}} - \left(2\xi_2 \xi_3 + \frac{1}{2} \xi_1^2 \xi_2 \right) \frac{e_{X1}}{|e_{X1}|} \\ &\quad + \left(2\xi_3 + \frac{1}{2} \xi_1^2 \right) \frac{e_{X1} e_{X2}}{|e_{X1}|} - (2\xi_1 \xi_4 + \xi_1 \xi_2^2) |e_{X1}|^{\frac{3}{2}} \\ &\quad - (2\xi_2 \xi_4 + \xi_2^3) e_{X1}^2 + (2\xi_4 + \xi_2^2) e_{X1} e_{X2} \\ &\quad - \frac{3}{2} \xi_1^2 \xi_2 |e_{X1}| - \frac{3}{2} \xi_1 \xi_2^2 |e_{X1}|^{\frac{3}{2}} + \frac{3}{2} \xi_1 \xi_2 \frac{e_{X1}}{|e_{X1}|^{\frac{1}{2}}} e_{X2} \\ &\quad + \xi_1 \xi_2 \frac{e_{X1}}{|e_{X1}|^{\frac{1}{2}}} e_{X2} + \xi_2^2 e_{X1} e_{X2} - \xi_2 e_{X2}^2 \\ &\quad + \xi_2 \xi_3 |e_{X1}| + \xi_2 \xi_4 e_{X1}^2 - \xi_2 e_{X1} \dot{d}_X \\ &\quad + \frac{1}{2} \xi_1^2 \frac{e_{X1}}{|e_{X1}|} e_{X2} + \frac{1}{2} \xi_1 \xi_2 \frac{e_{X1}}{|e_{X1}|^{\frac{1}{2}}} e_{X2} - \frac{1}{2} \xi_1 \frac{e_{X2}^2}{|e_{X1}|^{\frac{1}{2}}} \\ &\quad + \xi_1 \xi_3 |e_{X1}|^{\frac{1}{2}} + \xi_1 \xi_4 |e_{X1}|^{\frac{3}{2}} - \xi_1 \frac{e_{X1}}{|e_{X1}|^{\frac{1}{2}}} \dot{d}_X \end{aligned}$$

$$-2\xi_3 \frac{e_{x1}}{|e_{x1}|} e_{x2} - 2\xi_4 e_{x1} e_{x2} + 2e_{x2} \dot{d}_x. \tag{32}$$

Obviously, (32) is a complex polynomial equation. For convenience, we transform (32) in the following form

$$\begin{aligned} \dot{V}_x = & - \left(2\xi_1 \xi_3 + \frac{1}{2} \xi_1^3 \right) |e_{x1}|^{\frac{1}{2}} + \xi_1 \xi_3 |e_{x1}|^{\frac{1}{2}} \\ & - (2\xi_1 \xi_4 + \xi_1 \xi_2^2) |e_{x1}|^{\frac{3}{2}} - \frac{3}{2} \xi_1 \xi_2^2 |e_{x1}|^{\frac{3}{2}} \\ & + \xi_1 \xi_4 |e_{x1}|^{\frac{3}{2}} + \left(2\xi_3 + \frac{1}{2} \xi_1^2 \right) \frac{e_{x1} e_{x2}}{|e_{x1}|} \\ & + \frac{1}{2} \xi_1^2 \frac{e_{x1}}{|e_{x1}|} e_{x2} - 2\xi_3 \frac{e_{x1}}{|e_{x1}|} e_{x2} \\ & + \frac{3}{2} \xi_1 \xi_2 \frac{e_{x1}}{|e_{x1}|^{\frac{1}{2}}} e_{x2} + \xi_1 \xi_2 \frac{e_{x1}}{|e_{x1}|^{\frac{1}{2}}} e_{x2} \\ & + \frac{1}{2} \xi_1 \xi_2 \frac{e_{x1}}{|e_{x1}|^{\frac{1}{2}}} e_{x2} - \left(2\xi_2 \xi_3 + \frac{1}{2} \xi_1^2 \xi_2 \right) \frac{e_{x1}^2}{|e_{x1}|} \\ & - \frac{3}{2} \xi_1^2 \xi_2 |e_{x1}| + \xi_2 \xi_3 |e_{x1}| \\ & + (2\xi_4 + \xi_2^2) e_{x1} e_{x2} + \xi_2^2 e_{x1} e_{x2} - 2\xi_4 e_{x1} e_{x2} \\ & - \frac{1}{2} \xi_1 \frac{e_{x2}^2}{|e_{x1}|^{\frac{1}{2}}} - (2\xi_2 \xi_4 + \xi_2^3) e_{x1}^2 + \xi_2 \xi_4 e_{x1}^2 \\ & - \xi_2 e_{x2}^2 + 2e_{x2} \dot{d}_x - \xi_2 e_{x1} \dot{d}_x - \xi_1 \frac{e_{x1}}{|e_{x1}|^{\frac{1}{2}}} \dot{d}_x. \end{aligned} \tag{33}$$

Furthermore, (33) follows from $|\dot{d}_x| \leq \delta_x, e_{x1} \leq |e_{x1}|$ and $e_{x2} \leq |e_{x2}|$ that

$$\begin{aligned} \dot{V}_x \leq & - \left(\xi_1 \xi_3 + \frac{1}{2} \xi_1^3 \right) |e_{x1}|^{\frac{1}{2}} - \left(\xi_1 \xi_4 + \frac{5}{2} \xi_1 \xi_2^2 \right) |e_{x1}|^{\frac{3}{2}} \\ & - \frac{\xi_1}{2} \frac{e_{x2}^2}{|e_{x1}|^{\frac{1}{2}}} + \xi_1^2 |e_{x2}| + 3\xi_1 \xi_2 |e_{x1}|^{\frac{1}{2}} |e_{x2}| \\ & - (\xi_2 \xi_3 + 2\xi_1^2 \xi_2) |e_{x1}| - (\xi_2 \xi_4 + \xi_2^3) |e_{x1}|^2 \\ & - \xi_2 |e_{x2}|^2 + 2\xi_2^2 |e_{x1}| |e_{x2}| + 2\delta_x |e_{x2}| \\ & + \xi_2 \delta_x |e_{x1}| + \xi_1 \delta_x |e_{x1}|^{\frac{1}{2}}. \end{aligned} \tag{34}$$

Define $\Pi_x = [|e_{x1}|^{\frac{1}{2}}, e_{x1}, e_{x2}]^T$. Then (34) can be rewritten as

$$\dot{V}_x \leq - \frac{1}{|e_{x1}|^{\frac{1}{2}}} \Pi_x^T \Lambda_{x1} \Pi_x - \Pi_x^T \Lambda_{x2} \Pi_x, \tag{35}$$

where

$$\begin{aligned} \Lambda_{x1} &= \frac{1}{2} \begin{bmatrix} 2\xi_1 \xi_3 + \xi_1^3 - 2\xi_1 \delta_x & 0 & -\xi_1^2 - 2\delta_x \\ 0 & 2\xi_1 \xi_4 + 5\xi_1 \xi_2^2 & -3\xi_1 \xi_2 \\ -\xi_1^2 - 2\delta_x & -3\xi_1 \xi_2 & \xi_1 \end{bmatrix}, \end{aligned}$$

$$\Lambda_{x2} = \begin{bmatrix} \xi_2 \xi_3 + 2\xi_1^2 \xi_2 - \xi_2 \delta_x & 0 & 0 \\ 0 & \xi_2 \xi_4 + \xi_2^3 - \xi_2^2 & \\ 0 & -\xi_2^2 & \xi_2 \end{bmatrix},$$

If the matrices Λ_{x1} and Λ_{x2} are positive definite, i.e., the following inequality holds,

$$\begin{cases} \xi_1 \xi_3 + \frac{\xi_1^3}{2} - \xi_1 \delta_x > 0, \\ \langle \Sigma_{x1} \rangle > 0, \\ \xi_2 \xi_3 + 2\xi_1^2 \xi_2 - \xi_2 \delta_x > 0, \\ \langle \Sigma_{x2} \rangle > 0, \end{cases} \tag{36}$$

where $\langle \cdot \rangle$ denotes the determinant of matrix \cdot , then (35) can be derived as

$$\dot{V}_x \leq - \frac{1}{|e_{x1}|^{\frac{1}{2}}} \Pi_x^T \Lambda_{x1} \Pi_x. \tag{37}$$

Notice that (29) can be written as:

$$V_x = \Theta_x^T \Gamma_x \Theta_x, \tag{38}$$

where

$$\Theta_x = \begin{bmatrix} |e_{x1}|^{\frac{1}{2}} \text{sign}(e_{x1}) \\ e_{x1} \\ e_{x2} \end{bmatrix},$$

and

$$\Gamma_x = \frac{1}{2} \begin{bmatrix} 4\xi_3 + \xi_1^2 & \xi_1 \xi_2 & -\xi_1 \\ \xi_1 \xi_2 & 2\xi_4 + \xi_2^2 & -\xi_2 \\ -\xi_1 & -\xi_2 & 2 \end{bmatrix}.$$

by simply calculating, we have $\Pi_x^T \Pi_x = \Theta_x^T \Theta_x$. According to (37) and Lemma 3, it is obtained that

$$\begin{aligned} \dot{V}_x &\leq - \frac{1}{|e_{x1}|^{\frac{1}{2}}} \lambda_{\min}(\Lambda_{x1}) \Pi_x^T \Pi_x \\ &\leq - \frac{1}{|e_{x1}|^{\frac{1}{2}}} \lambda_{\min}(\Lambda_{x1}) \Theta_x^T \Theta_x. \end{aligned} \tag{39}$$

Meanwhile, by virtue of Lemma 3, we get from (38)

$$\begin{aligned} \Theta_x^T \Theta_x &\geq \frac{\Theta_x^T \Gamma_x \Theta_x}{\lambda_{\max}(\Gamma_x)} \\ &\geq \frac{V_x}{\lambda_{\max}(\Gamma_x)}, \end{aligned} \tag{40}$$

and

$$\begin{aligned} \lambda_{\min}(\Gamma_x) (\Theta_x^T \Theta_x) &\leq \Theta_x^T \Gamma_x \Theta_x \\ &\leq V_x, \end{aligned} \tag{41}$$

i.e.,

$$\begin{aligned} V_x^{\frac{1}{2}} &\geq \sqrt{\lambda_{\min}(\Gamma_x) (\Theta_x^T \Theta_x)^{\frac{1}{2}}} \\ &\geq \sqrt{\lambda_{\min}(\Gamma_x) |e_{x1}|^{\frac{1}{2}}}. \end{aligned} \tag{42}$$

(42) can be further rewritten as

$$\frac{1}{|e_{\chi 1}|^{\frac{1}{2}}} \geq \frac{\sqrt{\lambda_{\min}(\Gamma_{\chi})}}{V_{\chi}^{\frac{1}{2}}}. \tag{43}$$

Using (39) and (40), one has

$$\dot{V}_{\chi} \leq -\frac{1}{|e_{\chi 1}|^{\frac{1}{2}}} \lambda_{\min}(\Lambda_{\chi 1}) \frac{V_{\chi}}{\lambda_{\max}(\Gamma_{\chi})}. \tag{44}$$

Combining (43) and (44), it is obtained that:

$$\dot{V}_{\chi} \leq -\rho_{\chi} V_{\chi}^{\frac{1}{2}}, \tag{45}$$

where

$$\rho_{\chi} = \frac{\lambda_{\min}(\Lambda_{\chi 1}) \sqrt{\lambda_{\min}(\Gamma_{\chi})}}{\lambda_{\max}(\Gamma_{\chi})} > 0.$$

By comparing Lemma 1 it follows easily that V_{χ} with initial value $V_{\chi}(0)$, $e_{\chi 1}$ and $e_{\chi 2}$ will converge to zero in finite time and the reaching time is given by

$$T_{\chi} \leq \frac{2V_{\chi}^{\frac{1}{2}}(0)}{\rho_{\chi}}, \tag{46}$$

which indicates the $e_{\chi 1}$ and $e_{\chi 2}$ will converge to zero in finite time. Then, term $\hat{d}_{\chi} - d_{\chi}$ in (28) will vanish at $t \geq T_{\chi}$. Therefore, (28) can be rewritten as

$$\dot{\tilde{V}}_{\chi} = -c_{\chi} E_{\chi}^2 + E_{\chi} \tilde{E}_{\chi} + s_{\chi} (-E_{\chi} - h_{\chi} s_{\chi}). \tag{47}$$

According to (16), $\tilde{E}_{\chi} = s_{\chi} - n_{\chi} E_{\chi}$. Thereby, (47) is further derived as

$$\begin{aligned} \dot{\tilde{V}}_{\chi} &= -c_{\chi} E_{\chi}^2 + E_{\chi} (s_{\chi} - n_{\chi} E_{\chi}) - s_{\chi} E_{\chi} - h_{\chi} s_{\chi}^2 \\ &= -c_{\chi} E_{\chi}^2 - n_{\chi} E_{\chi}^2 - h_{\chi} s_{\chi}^2 \\ &\leq -\lambda_{\chi} \tilde{V}_{\chi}, \end{aligned} \tag{48}$$

where $\lambda_{\chi} = \min\{2(c_{\chi} + n_{\chi}), 2h_{\chi}\}$. Note that $\min\{a, b\}$ means to select the minimum from a and b . Using Lemma 2, we have

$$\tilde{V}_{\chi} \leq \tilde{V}_{\chi}(0) e^{-\lambda_{\chi} t}, t \geq 0, \tag{49}$$

where $\tilde{V}_{\chi}(0)$ is the initial value of \tilde{V}_{χ} . Obviously, the tracking error E_{χ} will converge to zero asymptotically from (24) and (49).

In the following, we will derive the bound of the attitude transient tracking error in terms of L_2 norm. From the definition of \tilde{V}_{χ} (24)

$$\frac{1}{2} E_{\chi}^2 + \frac{1}{2} s_{\chi}^2 \leq \tilde{V}_{\chi}(0) e^{-\lambda_{\chi} t}. \tag{50}$$

According to (12), (13), (14) and (16), s_{χ}^2 can be expressed by

$$\begin{aligned} s_{\chi} &= n_{\chi} E_{\chi} + \tilde{E}_{\chi} \\ &= n_{\chi} E_{\chi} + c_{\chi} E_{\chi} + \dot{\chi} d - \dot{\chi} \\ &= n_{\chi} E_{\chi} + c_{\chi} E_{\chi} + \dot{E}_{\chi}. \end{aligned} \tag{51}$$

Substituting (51) into (50), we have

$$\begin{aligned} \tilde{V}_{\chi}(0) e^{-\lambda_{\chi} t} &\geq \frac{1}{2} E_{\chi}^2 + \frac{1}{2} (n_{\chi} E_{\chi} + c_{\chi} E_{\chi} + \dot{E}_{\chi})^2 \\ &= \frac{1}{2} E_{\chi}^2 + \frac{1}{2} (n_{\chi} + c_{\chi})^2 E_{\chi}^2 + \frac{1}{2} (\dot{E}_{\chi})^2 \\ &\quad + (n_{\chi} + c_{\chi}) E_{\chi} \dot{E}_{\chi}. \end{aligned} \tag{52}$$

Integrating both sides of (52) yields

$$\begin{aligned} \int_0^{\infty} \tilde{V}_{\chi}(0) e^{-\lambda_{\chi} t} dt &\geq \int_0^{\infty} \left(\left(\frac{1}{2} + \frac{1}{2} (n_{\chi} + c_{\chi})^2 \right) E_{\chi}^2 \right. \\ &\quad \left. + \frac{1}{2} (\dot{E}_{\chi})^2 + (n_{\chi} + c_{\chi}) E_{\chi} \dot{E}_{\chi} \right) dt \\ &= \int_0^{\infty} \left(\frac{1}{2} + \frac{1}{2} (n_{\chi} + c_{\chi})^2 \right) E_{\chi}^2 dt \\ &\quad + \int_0^{\infty} (n_{\chi} + c_{\chi}) E_{\chi} \dot{E}_{\chi} dt \\ &\quad + \int_0^{\infty} \frac{1}{2} (\dot{E}_{\chi})^2 dt. \end{aligned} \tag{53}$$

Note that according to the definition of L_2 norm, the expression of $\|E_{\chi}\|_2$ is

$$\|E_{\chi}\|_2 = \sqrt{\int_0^{\infty} \|E_{\chi}\|^2 dt}, \tag{54}$$

where $\|E_{\chi}\|$ is defined as Euclidean norm of E_{χ} , given by

$$\|E_{\chi}\| = \sqrt{E_{\chi} E_{\chi}}. \tag{55}$$

Hence, (53) implies

$$\begin{aligned} \frac{1}{\lambda_{\chi}} \tilde{V}_{\chi}(0) &\geq \left(\frac{1}{2} + \frac{1}{2} (n_{\chi} + c_{\chi})^2 \right) \|E_{\chi}\|_2^2 \\ &\quad + \frac{1}{2} (n_{\chi} + c_{\chi}) (E_{\chi}^2(\infty) - E_{\chi}^2(0)) \\ &\quad + \int_0^{\infty} \frac{1}{2} (\dot{E}_{\chi})^2 dt. \end{aligned} \tag{56}$$

From (49), $E_{\chi}(\infty) \rightarrow 0$, i.e., $E_{\chi}^2(\infty) \rightarrow 0$. If we set all initial states of the quadrotor system to be zero, we have $\chi(0) = \dot{\chi}(0) = 0$, where $\chi(0)$ and $\dot{\chi}(0)$ denote initial values of χ and its derivative, respectively. Therefore,

$E_\chi(0) = \chi_d(0) - \chi(0) = \chi_d(0)$ from (12). Furthermore, (56) can be written as

$$\frac{1}{\lambda_\chi} \bar{V}_\chi(0) \geq \left(\frac{1}{2} + \frac{1}{2}(n_\chi + c_\chi)^2 \right) \|E_\chi\|_2^2 - \frac{1}{2}(n_\chi + c_\chi)\chi_d^2(0) + \frac{1}{2} \int_0^\infty (\dot{E}_\chi)^2 dt. \tag{57}$$

Next, we will calculate the improper integral $\int_0^\infty (\dot{E}_\chi)^2 dt$. To derive the convergence of $\int_0^\infty (\dot{E}_\chi)^2 dt$, we construct an auxiliary equation as

$$G_a(E_\chi) = \int_0^\infty (\dot{E}_\chi)^2 dt \int_0^\infty (\underline{e}^{-t})^2 dt. \tag{58}$$

Applying Cauchy–Schwarz inequality [43] to (58), we have

$$G_a(E_\chi) \geq \left(\int_0^\infty \dot{E}_\chi \underline{e}^{-t} dt \right)^2, \tag{59}$$

Let

$$g_1(t) = \underline{e}^{-t}, \tag{60}$$

and

$$g_2(t) = \dot{E}_\chi. \tag{61}$$

Obviously, $g_1(t)$ is a monotone function on $[0, \infty)$ and

$$\lim_{t \rightarrow \infty} g_1(t) = 0. \tag{62}$$

Moreover, $g_2(t)$ is integrable on $[0, c]$ for all $c > 0$, and the integral function $G_2(x) = \int_0^\infty g_2(t) dt$ is bounded on $[0, \infty]$. Therefore, the improper integral $\int_0^\infty \dot{E}_\chi \underline{e}^{-t} dt$ in (59) is convergent by comparing with Lemma 4. Let M_E be the convergent value of the improper integral $\int_0^\infty \dot{E}_\chi \underline{e}^{-t} dt$, then we get

$$\int_0^\infty \dot{E}_\chi \underline{e}^{-t} dt = M_E. \tag{63}$$

Combining (58), (59) and (63), the following inequality holds

$$\int_0^\infty (\dot{E}_\chi)^2 dt \int_0^\infty (\underline{e}^{-t})^2 dt \geq M_E^2. \tag{64}$$

Note that

$$\int_0^\infty (\underline{e}^{-t})^2 dt = \frac{1}{2}. \tag{65}$$

Substituting (65) into (64), it is obtained that

$$\int_0^\infty (\dot{E}_\chi)^2 dt \geq 2M_E^2. \tag{66}$$

Considering (66) and (57), it follows that

$$\|E_\chi\|_2^2 \leq \frac{2\bar{V}_\chi(0) + \lambda_\chi(n_\chi + c_\chi)\chi_d^2(0) - 2\lambda_\chi M_E^2}{\lambda_\chi + \lambda_\chi(n_\chi + c_\chi)^2}. \tag{67}$$

Thereby, the bound of the transient tracking error E_χ in terms of L_2 norm can be obtained by

$$\|E_\chi\|_2 \leq \sqrt{\frac{2\bar{V}_\chi(0) + \lambda_\chi(n_\chi + c_\chi)\chi_d^2(0) - 2\lambda_\chi M_E^2}{\lambda_\chi + \lambda_\chi(n_\chi + c_\chi)^2}}. \tag{68}$$

In addition, according to (24), $\bar{V}_\chi(0)$ is given by

$$\bar{V}_\chi(0) = \frac{1}{2} E_\chi^2(0) + \frac{1}{2} s_\chi^2(0). \tag{69}$$

From (12), we have

$$E_\chi^2(0) = (\chi_d(0) - \chi(0))^2 = \chi_d^2(0). \tag{70}$$

Using (51) and (70), we get

$$\begin{aligned} s_\chi^2(0) &= (n_\chi E_\chi(0) + c_\chi E_\chi(0) + \dot{E}_\chi(0))^2 \\ &= ((n_\chi + c_\chi)\chi_d(0) + \dot{\chi}_d(0))^2 \\ &= (n_\chi + c_\chi)^2 \chi_d^2(0) + (\dot{\chi}_d(0))^2 \\ &\quad + 2(n_\chi + c_\chi)\chi_d(0)\dot{\chi}_d(0). \end{aligned} \tag{71}$$

Substituting (70) and (71) into (69), $\bar{V}_\chi(0)$ is derived as

$$\bar{V}_\chi(0) = \chi_d^2(0) + (n_\chi + c_\chi)^2 \chi_d^2(0) + (\dot{\chi}_d(0))^2 + 2(n_\chi + c_\chi)\chi_d(0)\dot{\chi}_d(0). \tag{72}$$

Combining (68) and (72), we obtain

$$\|E_\chi\|_2 \leq \sqrt{\beta_{\chi 1} + \beta_{\chi 2} + \beta_{\chi 3} + \beta_{\chi 4}}, \tag{73}$$

where $\beta_{\chi i} = \Xi_{\chi i}, i = 1, \dots, 4$.

This completes the proof. \square

Remark 3 It is worth mentioning that although the signum function is involved in the Lyapunov function candidate, V_χ in (29) is a continuous function. In the following, we analyze the continuity on the left and right of the point $e_{\chi 1} = 0$ in the signum function.

- (i) When $e_{\chi 1} = 0$, it is easy to get $V_\chi = e_{\chi 1}^2$;
- (ii) When $e_{\chi 1} \rightarrow 0^-$, we obtain $|e_{\chi 1}|^{\frac{1}{2}} \text{sign}(e_{\chi 1}) \rightarrow 0^-$. Therefore, $V_\chi \rightarrow e_{\chi 1}^{2+}$;
- (iii) When $e_{\chi 1} \rightarrow 0^+$, we obtain $|e_{\chi 1}|^{\frac{1}{2}} \text{sign}(e_{\chi 1}) \rightarrow 0^+$. Therefore, $V_\chi \rightarrow e_{\chi 1}^{2-}$; Synthesizing (i), (ii) and (iii), it is concluded that (29) is a continuous function.

Remark 4 Note that the generalized Lyapunov theory only requires continuity and not differentiability of V_χ along the solution trajectories [44, 45]. Moreover, $e_{\chi 1}$ cannot be stabilized on the set $\{(e_{\chi 1}, e_{\chi 2}) \in \mathbb{R}^2 | e_{\chi 1} = 0\} \setminus (0, 0)$, since $\dot{e}_{\chi 1} = e_{\chi 2} \neq 0$ from the first equation in (11) if only $e_{\chi 1} = 0$. Therefore, the equilibrium point $e_{\chi 1} = e_{\chi 2} = 0$ can be reached in finite time.

Remark 5 The saturation function given by

$$y_{\text{output}} = \begin{cases} c_{\max}, & c_{\max} \leq x_{\text{input}}, \\ x_{\text{input}}, & c_{\min} < x_{\text{input}} < c_{\max}, \\ c_{\min}, & x_{\text{input}} \leq c_{\min}, \end{cases} \quad (74)$$

where x_{input} and y_{output} are the input and output of saturation function, respectively, and c_{\max} and c_{\min} are the upper bound and lower bound of saturation function, respectively, can be used to replace signum function in (10) to reduce chattering of the designed observer.

Remark 6 The consideration for the mechanism of the auxiliary equation. In the derivation of the L_2 norm bound of the tracking error, the determination of convergence of the improper integral $\int_0^\infty (\dot{E}_\chi)^2 dt$ is very important. Firstly, we need to introduce a related function according to the conditions in Lemma 4. Obviously, a potential function is $g_1(t) = e^{-t}$. Secondly, the relationship between the integral of the product of two functions and the integral of one of them can be found from Cauchy–Schwarz inequality. The above two ideas impel us to obtain the auxiliary equation (58) by repeated verification and trial and error.

Remark 7 The guideline for tuning of control parameters. Overall, the tuning parameters including the observer gains and the controller gains are obtained through trial and error based on tracking results. In the proposed controller, the control gains c_χ , n_χ and h_χ are easy to be determined, since the conditions of selection are relaxed. It is found that the values of the gains c_χ , n_χ and h_χ have a direct effect on the overshoot, tracking error and its convergence rate, but the effect of h_χ is the most obvious in all three channels. It is worth mentioning that the effect of c_χ , n_χ on the above three indexes is very weak in the pitch channel. In the designed observer, the first and third inequalities are relatively simple from the conditions (36). Therefore, we first choose suitable parameters ξ_1 and ξ_3 to satisfy the first inequality, then ξ_2 can be chosen from the third inequality. Finally, ξ_4 can be determined according to the second and fourth inequalities. We find that ξ_2 and

ξ_3 have a greater effect on the adaption mechanism of disturbance than ξ_1 and ξ_4 . Based on the above analysis and consideration, to obtain the better control parameters, h_χ , ξ_2 and ξ_3 should be tuned carefully, while c_χ , n_χ , ξ_1 and ξ_4 can be tuned roughly.

5 Simulation

The parameters of the quadrotor system are set as follows [46]: $I_x = 0.16 \text{ kg m}^2$, $I_y = 0.16 \text{ kg m}^2$, $I_z = 0.32 \text{ kg m}^2$, $L = 0.4 \text{ m}$, $f = 0.05 \text{ m}$. The initial attitude angles of the quadrotor are set as $[0 \ 0 \ 0]$ rad.

The quadrotor is required to track the following reference signals:

$$\phi_d = \begin{cases} 0.1 - \sqrt{0.1^2(1 - \frac{t^2}{12^2})}, & 0 \leq t \leq 12, \\ 0.1 + \sqrt{0.1^2(1 - \frac{(t-16)^2}{4^2})}, & 12 < t \leq 20, \end{cases} \quad (75)$$

$$\theta_d = 0.1 \cos(\frac{\pi}{3}t + \frac{\pi}{4}) + 0.2 \sin(0.35t + 0.27) + 0.2, \quad (76)$$

$$\phi_d = \begin{cases} 0.012(t - 4.5)^2, & 0 \leq t \leq 10, \\ \frac{3.63}{t}, & 10 < t \leq 20, \end{cases} \quad (77)$$

where the desired signal in the roll channel is an elliptical trajectory [47]. The external disturbances acting on the quadrotor are set as

$$d_\phi = 0.78e^{-\frac{t}{4}}(\frac{t-1}{2})^2 + \tanh(3t + 0.35), \quad (78)$$

$$d_\theta = \begin{cases} 0.017(t-5)^3 + 0.1, & 0 \leq t \leq 8, \\ -0.38(t-20), & 8 < t \leq 20, \end{cases} \quad (79)$$

$$d_\psi = \begin{cases} 0, & 0 \leq t \leq 3, \\ 1.21(1 - \sin(2\pi\frac{t-3}{13})), & 3 < t \leq 16, \\ \frac{650}{(t-2)^2} + 0.28, & 16 < t \leq 20. \end{cases} \quad (80)$$

5.1 Compared with other FTDO

A comparative simulation with the FTDO in [13, 16] is carried out to highlight the observation performance of the proposed FTDO.

The observation results and observation errors for the external disturbances (78)–(80) are shown in Figs. 2 and 3, respectively. It can be seen that the given disturbances can be estimated online by the two observers, which indicates that the compensation for the disturbances can be effectively achieved in the controllers

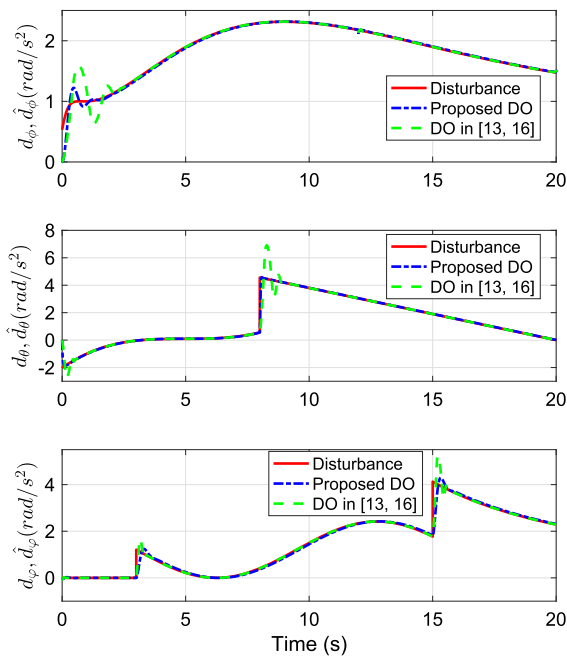


Fig. 2 The observation results for the given disturbances

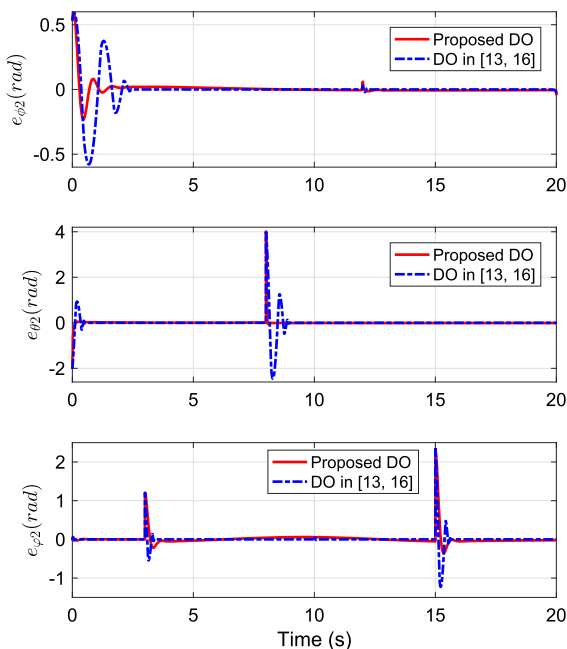


Fig. 3 The observation errors for the given disturbances

(18). However, the observation result in the roll channel have oscillations at the initial stage when using the FTDO in [13,16]. Meanwhile, the observation results obtained by the FTDO in [13,16] have greater over-

Table 2 The quantitative evaluations of the observation errors

Index	Roll channel	Pitch channel	Yaw channel
MAE (Proposed)	0.0176	0.0174	0.0543
MAE ([13,16])	0.0316	0.0703	0.0276
RMSE (Proposed)	0.0589	0.1313	0.1779
RMSE ([13,16])	0.1127	0.3595	0.1715
SDE (Proposed)	0.0587	0.1313	0.1776
SDE ([13,16])	0.1127	0.3595	0.1715

shoot when the disturbance is switched in the pitch and yaw channels.

To quantitatively evaluate the observation performance of the two FTDOs, the indexes including the mean value of absolute value of the error (MAE), the root mean square of the error (RMSE) and the standard deviation of the error (SDE) are used. The indexes MAE and RMSE are used to measure the accuracy of the observation/tracking error, while the index SDE is used to measure the degree of oscillation of the observation/tracking results. Note that the evaluation of index SDE is based on indexes MAE and RMSE. The values of the MAE, RMSE and SDE of the two observers are listed in Table 2. It can be seen that the MAE, RMSE and SDE of the proposed FTDO are smaller than that of the FTDO in [13,16] in the roll and pitch channels. In the yaw channel, the MAE of the FTDO in [13,16] is obviously smaller than that of the proposed observer, while the RMSE and SDE are roughly equal.

5.2 Compared with pure BSSMC without FTDO

To illustrate the effectiveness of the designed FTDO on the control performance, a comparative simulation between the proposed BSSMC with the FTDO and the pure BSSMC without the FTDO is performed. According to the designed controller (18), the BSSMC scheme without the FTDO can be derived as

$$F_{\chi} = T_{\chi}(n_{\chi}(-c_{\chi}E_{\chi} + \tilde{E}_{\chi}) + \dot{k}_{\chi} - G_{\chi} + E_{\chi} + h_{\chi}s_{\chi}). \tag{81}$$

It is worth mentioning that the controller gains c_{χ} , n_{χ} and h_{χ} of the two controllers are chosen to be the same.

The control inputs provided by the two controllers are depicted in Fig. 4. The tracking results for the desired attitude signals (75)–(77) are shown in Fig. 5, where we find that the tracking result for the desired

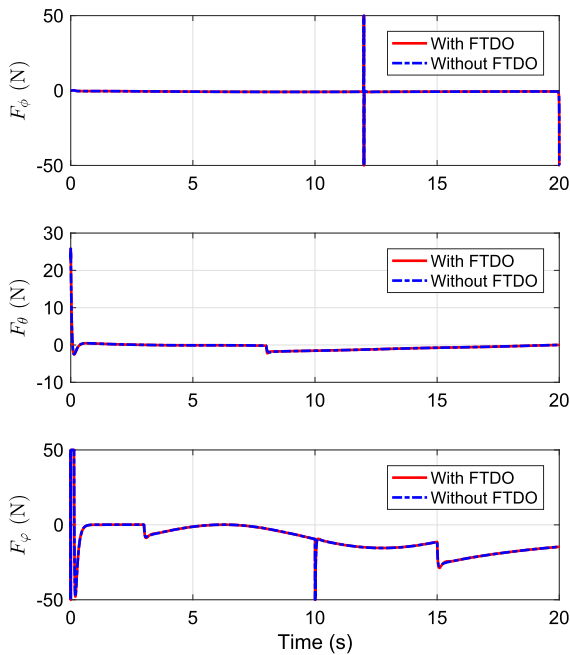


Fig. 4 The control inputs with/without the designed FTDO

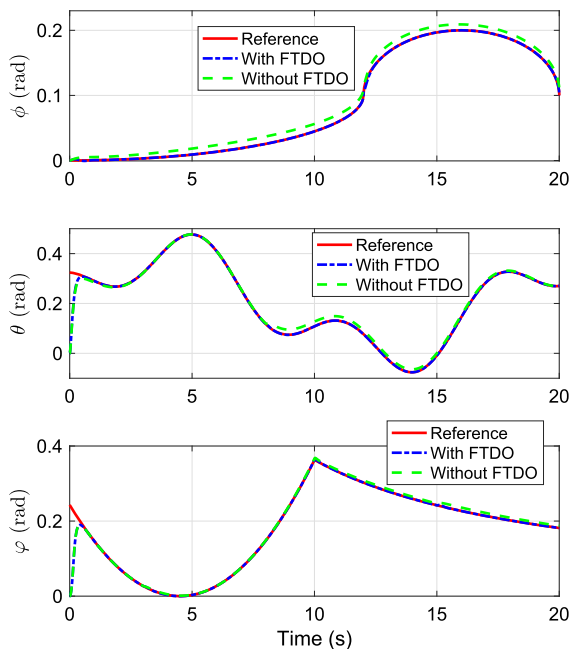


Fig. 5 The tracking results for the attitude angles

yaw attitude trajectory (77) is good. However, an obvious steady-state tracking error is produced when using the pure BSSMC in the roll channel. There is also a small tracking error produced by the pure BSSMC between 8 s and 12 s in the pitch channel. On the

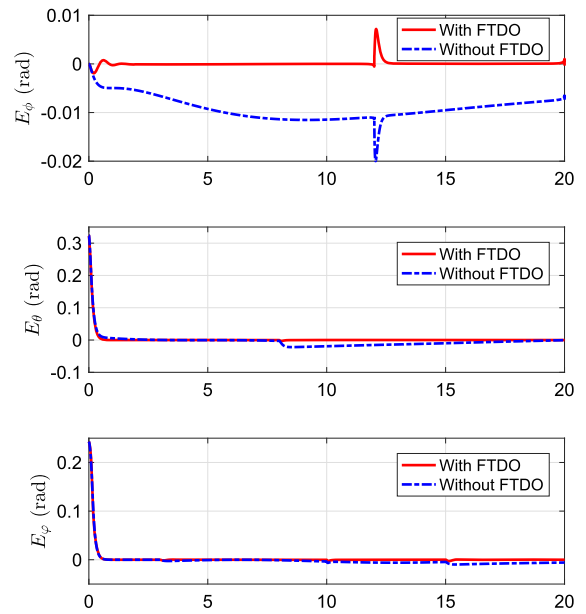


Fig. 6 The tracking errors for the attitude angles

contrary, the proposed controller synthesized with the FTDO can ensure that the desired attitude signals are closely followed in the three channels. The corresponding tracking errors of three attitude angles are plotted in Fig. 6.

In this quantitative evaluation, in addition to the indexes MAE, RMSE and SDE, we also consider the sum of square of control signal (SSC) as a measure of the energy consumed in the tracking of the reference trajectories. It should be noted that all four indexes need to be considered to comprehensively evaluate the advantages of the proposed control scheme. The MAE, RMSE, SDE and SSC are listed in Table 3, where we find that the performance of the BSSMC with the FTDO are better than that of the pure BSSMC in all four indexes in the roll channel. Besides, it is worth noting that the MAE of the BSSMC with the FTDO is smaller than half of that of the pure BSSMC in the case of roughly equal energy consumption in the pitch and yaw channels. These statistical results show that the designed FTDO has a positive effect on the tracking performance of the quadrotor system.

5.3 Compared with adaptive finite-time SMC in [11]

The following uncertainties in physical parameter are considered in the proposed control scheme, then a com-

Table 3 The quantitative evaluations of the tracking errors and control inputs using BSSMC with/without the FTDO

Index	Roll channel	Pitch channel	Yaw channel
MAE (With DO)	1.6507×10^{-4}	0.0026	0.0024
MAE (Without DO)	0.0091	0.0100	0.0060
RMSE (With DO)	6.5146×10^{-4}	0.0220	0.0196
RMSE (Without DO)	0.0094	0.0246	0.0202
SDE (With DO)	6.4888×10^{-4}	0.0219	0.0194
SDE (Without DO)	0.0024	0.0243	0.0201
SSC (With DO)	3.7740×10^4	2.5241×10^4	3.6684×10^6
SSC (Without DO)	3.7742×10^4	2.4883×10^4	3.6676×10^6

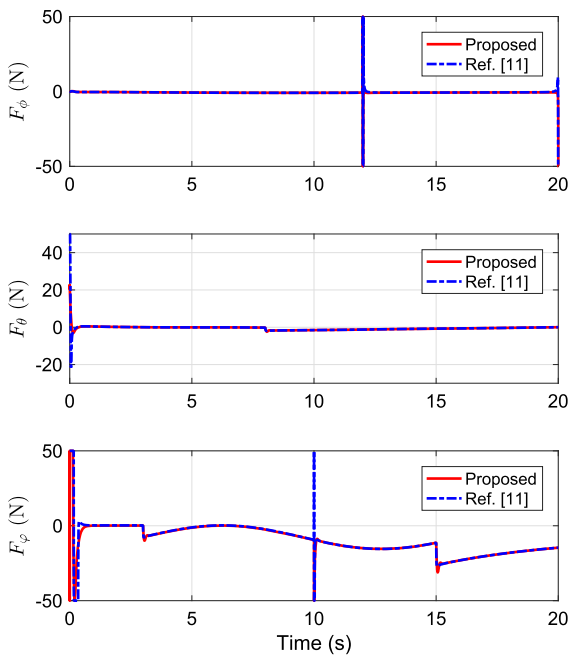


Fig. 7 The output signals of the two controllers

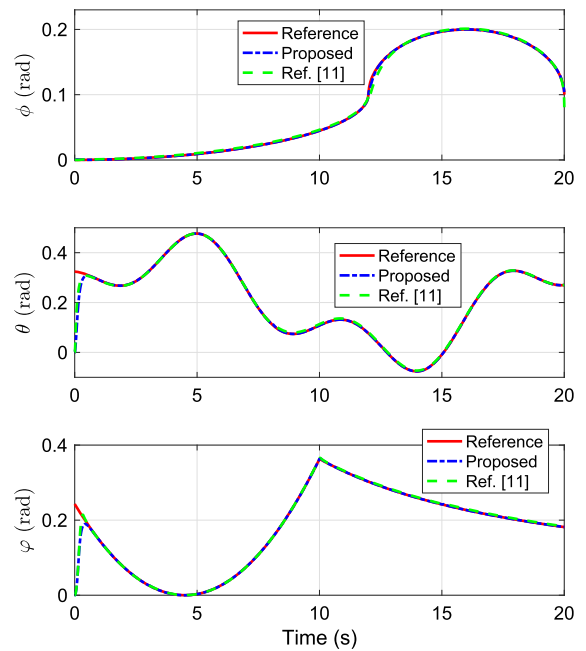


Fig. 8 The tracking results for the attitude angles

parative simulation with the controller in [11] is performed under the external disturbances (78)–(80).

$$\bar{I}_\alpha = 80\%I_\alpha, \alpha = x, y, z, \quad \bar{L} = 90\%L, \quad \bar{f} = 90\%f. \tag{82}$$

The outputs of the two controller are shown in Fig. 7. The corresponding tracking results and tracking errors are plotted in Figs. 8 and 9, respectively. It can be observed from Figs. 8 and 9 that the tracking performance of the proposed controller is slightly better than that of the controller in [11] in the roll channel, while a similar tracking performance is obtained by the two controller in the pitch and yaw channels.

The MAE, RMSE, SDE and SSC of the two control algorithms are given in Table 4. In the roll channel, the values of the four indexes of the proposed controller are smaller than that of the controller in [11], especially the energy required by the proposed controller is much less than that of the controller in [11]. In the pitch channel, much more energy is consumed by the control scheme in [11], but it is only slightly better than the proposed controller in indexes RMSE and SDE. In the yaw channel, the comprehensive performance of the two controllers is roughly equal by evaluating the four indexes.

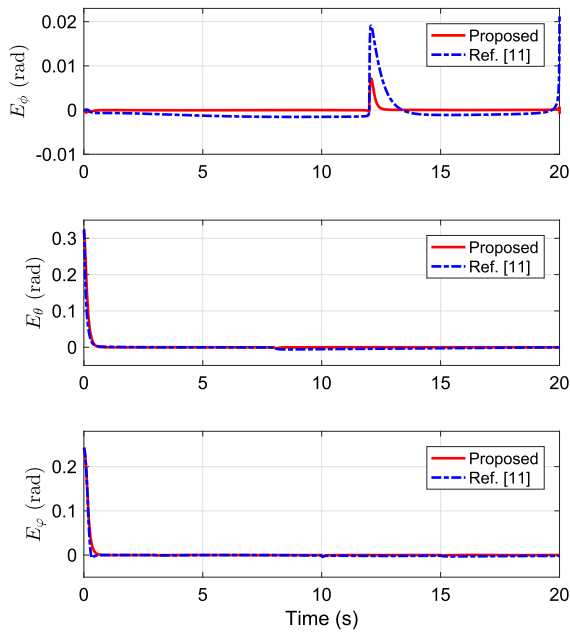


Fig. 9 The tracking errors for the attitude angles

5.4 Compared with LQR in [6]

Moreover, we consider the comparison between the proposed controller and LQR in terms of the tracking performance for the reference trajectories (75)–(77) in the presence of the external disturbances (78)–(80) and the white Gaussian noise [48]. Note that a weak noise and a strong noise are applied to the feedback channel of the closed-loop system respectively, which are subject to $X \sim \aleph(0, 0.000001)$ and $X \sim \aleph(0, 0.00002)$, where X denotes noise signal, \aleph denotes Gaussian distribution, 0 is the mean of the distribution, 0.000001 and 0.00002 are the covariance of the distribution.

Table 4 The quantitative evaluations of the tracking errors and control inputs using the proposed controller and the controller in [11]

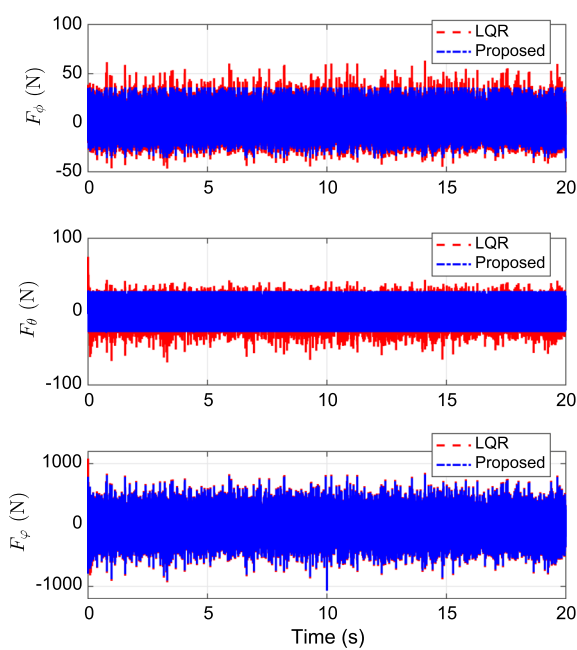
Index	Roll channel	Pitch channel	Yaw channel
MAE (Proposed)	1.1643×10^{-4}	0.0026	0.0024
MAE ([11])	0.0015	0.0037	0.0032
RMSE (Proposed)	6.2612×10^{-4}	0.0221	0.0196
RMSE ([11])	0.0027	0.0177	0.0191
SDE (Proposed)	6.2176×10^{-4}	0.0220	0.0194
SDE ([11])	0.0026	0.0177	0.0191
SSC (Proposed)	3.5516×10^4	2.4473×10^4	3.6792×10^6
SSC ([11])	8.3918×10^4	8.4003×10^4	3.9608×10^6

The control inputs, tracking results and tracking errors for the three desired attitude angles under the noise are depicted in Figs. 10, 11 and 12, respectively. It should be noted that in order to fairly compare the tracking performance of the two control algorithms, their SSCs should be as close as possible. In this sense, a saturation operator is applied to the roll and pitch controllers of the quadrotor. When there is a weak noise in the feedback channel, the tracking of reference trajectories (75)–(77) can be achieved by both controllers under the defined disturbances (78)–(80). However, the tracking performance in the roll channel decreases more significantly as the noise increases. Meanwhile, the tracking error in the pitch channel increases slightly when LQR is applied to the quadrotor from Fig. 12.

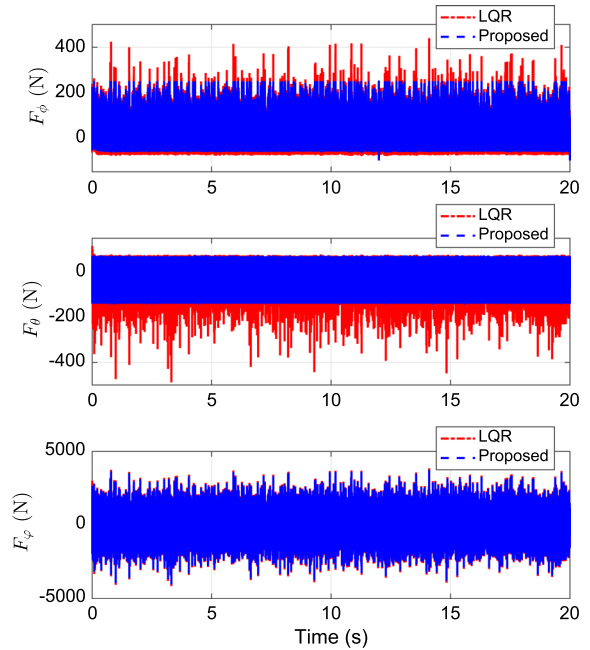
According to the above results, the MAE, RMSE, SDE and SSC under the weak and strong noises are shown in Tables 5 and 6, respectively. When the noise increases, these indexes become worse, especially the value of the SSC increases significantly. This means that the quadrotor system needs to receive more energy to maintain a stable tracking performance. It is worth pointing out that the tracking performance of the roll channel degrades fastest when the strong noise is applied to the quadrotor system. Overall, the proposed controller outperforms LQR in the terms of comprehensive performance from the comparative results in Figs. 10, 11 and 12 and the statistical results in Tables 5 and 6.

6 Conclusion

This article investigates the robust attitude trajectory tracking problem of a quadrotor drone in the pres-

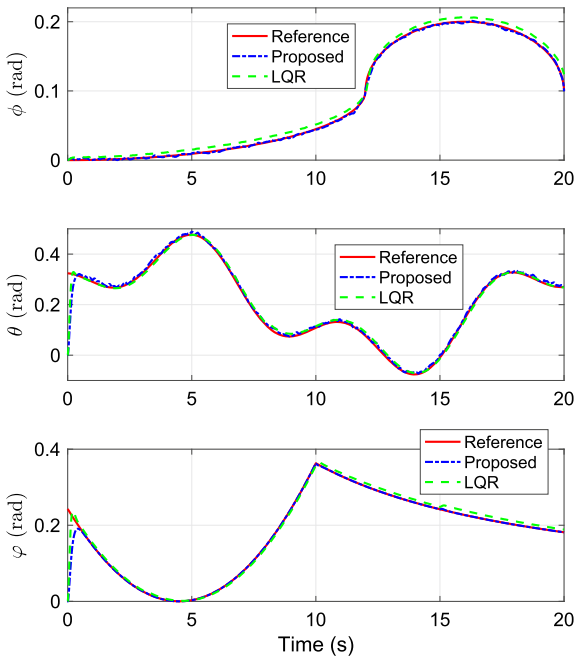


(a) The control inputs under the weak noise

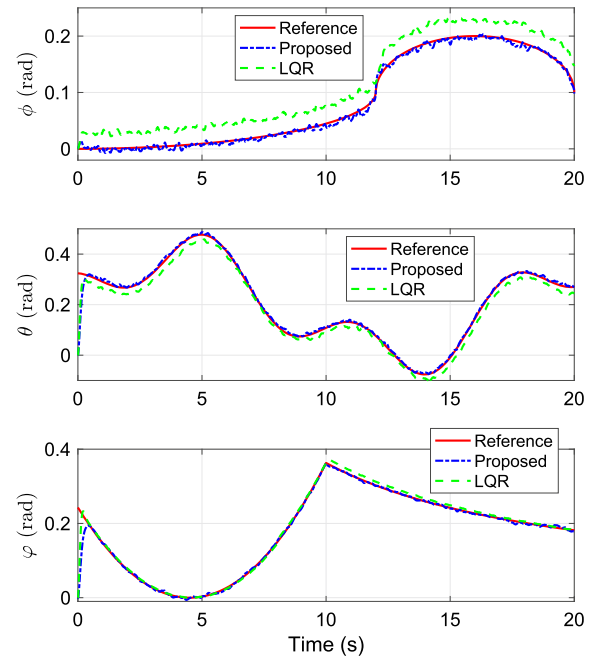


(b) The control inputs under the strong noise

Fig. 10 The control inputs of the two controllers under the noise



(a) The tracking results under the weak noise



(b) The tracking results under the strong noise

Fig. 11 The tracking results of the two controllers under the noise

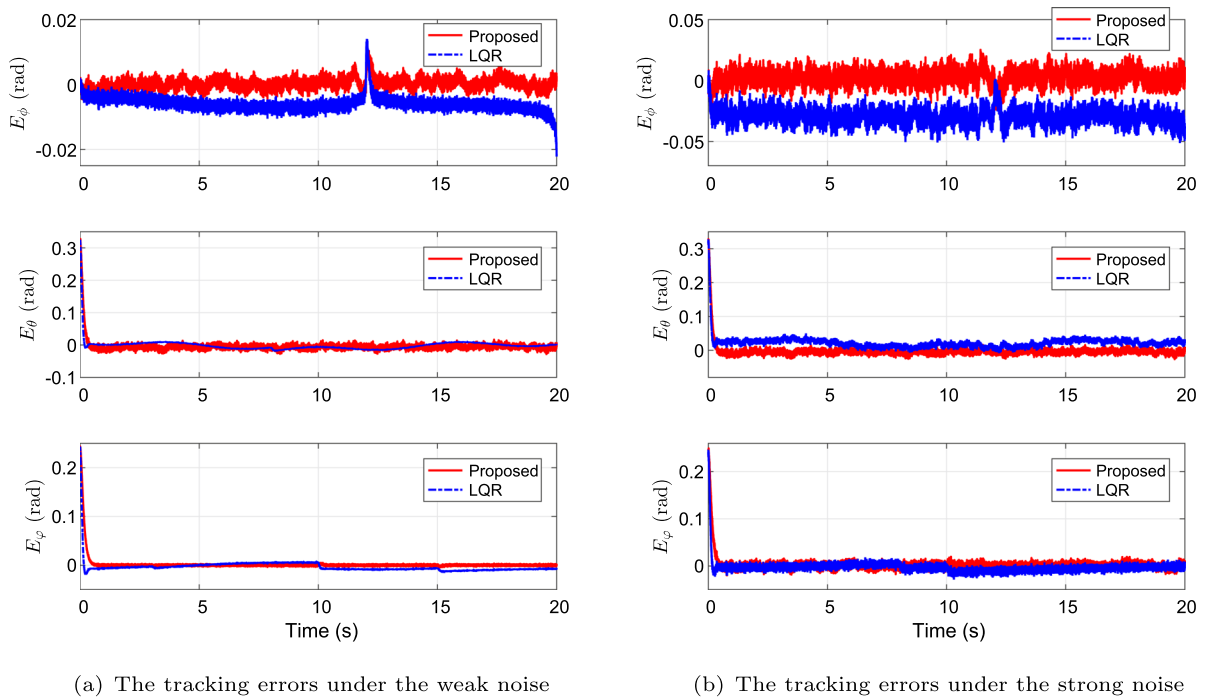


Fig. 12 The tracking errors of the two controllers under the noise

Table 5 The quantitative evaluations of the tracking errors and control signals using the proposed controller and LQR under the small noise

Index	Roll channel	Pitch channel	Yaw channel
MAE (Proposed)	0.0013	0.0038	0.0028
MAE (LQR)	0.0061	0.0083	0.0074
RMSE (Proposed)	0.0017	0.0221	0.0173
RMSE (LQR)	0.0064	0.0192	0.0145
SDE (Proposed)	0.0017	0.0221	0.0172
SDE (LQR)	0.0023	0.0191	0.0141
SSC (Proposed)	3.6347×10^6	4.8292×10^6	1.1105×10^9
SSC (LQR)	4.6122×10^6	4.6885×10^6	1.1837×10^9

Table 6 The quantitative evaluations of the tracking errors and control signals using the proposed controller and LQR under the strong noise

Index	Roll channel	Pitch channel	Yaw channel
MAE (Proposed)	0.0050	0.0087	0.0059
MAE (LQR)	0.0294	0.0221	0.0069
RMSE (Proposed)	0.0063	0.0226	0.0179
RMSE (LQR)	0.0300	0.0289	0.0147
SDE (Proposed)	0.0061	0.0223	0.0177
SDE (LQR)	0.0062	0.0187	0.0144
SSC (Proposed)	8.3871×10^7	9.8478×10^7	2.2112×10^{10}
SSC (LQR)	1.0482×10^8	1.0481×10^8	2.3502×10^{10}

ence of external disturbance. A nonlinear disturbance observer with finite-time convergence is proposed to estimate external disturbance. Then, a backstepping sliding mode control strategy based on the designed disturbance observer is proposed to guarantee the tracking errors of the three attitude angles of quadrotor to converge to zero asymptotically. In addition, the bound of the attitude transient tracking error in terms of L_2 norm is derived by constructing an auxiliary equation. The comparative simulations are carried out to verify the effectiveness of the proposed control scheme and several statistical indexes are used to quantitatively evaluate the performance in terms of observation error, tracking error and control signal. However, there exist two limitations in the proposed method: (1) the bound of disturbance's derivative needs to be known in the stability analysis of closed-loop systems and (2) the chattering phenomenon could occur in the designed disturbance observer. In future work, we will focus on the estimation of bound of disturbance's derivative and the suppress of chattering phenomenon.

Funding This work is supported in part by the National Natural Science Foundation of China (under Grant Nos. 51939001, 61976033); the Liaoning Revitalization Talents Program (under Grant No. XLYC1908018).

Data availability The datasets generated and/or analyzed during this study are available from the corresponding author on reasonable request.

Declaration

Conflict of interest The authors declare that they have no conflict of interest.

References

- Ghadiok, V., Goldin, J., Ren, W.: On the design and development of attitude stabilization, vision-based navigation, and aerial gripping for a low-cost quadrotor. *Auton. Robot.* **33**, 41–68 (2012)
- Zhao, L., Dai, L., Xia, Y., Li, P.: Attitude control for quadrotors subjected to wind disturbances via active disturbance rejection control and integral sliding mode control. *Mech. Syst. Signal Process.* **129**, 531–545 (2019)
- Lyu, X., Zhou, J., Gu, H., Li, Z., Shen, S., Zhang, F.: Disturbance observer based hovering control of quadrotor tail-sitter VTOL UAVs using H_∞ synthesis. *IEEE Robot. Autom. Lett.* **3**(4), 2910–2917 (2018)
- Eskandarpour, A., Sharf, I.: A constrained error-based MPC for path following of quadrotor with stability analysis. *Nonlinear Dyn.* **99**, 899–918 (2020)
- Dydek, Z.T., Annaswamy, A.M., Lavretsky, E.: Adaptive control of quadrotor UAVs: a design trade study with flight evaluations. *IEEE Trans. Control Syst. Technol.* **21**(4), 1400–1406 (2013)
- Koksal, N., Jalalmaab, M., Fidan, B.: Adaptive linear quadratic attitude tracking control of a quadrotor UAV based on IMU sensor data fusion. *Sensors* **19**(46), 1–23 (2019)
- Abro, G.E.M., Zulkifli, S.A.B.M., Asirvadani, V.S.: Dual-loop single dimension fuzzy-based sliding mode control design for robust tracking of an underactuated quadrotor craft. *Asian J. Control* **25**(1), 144–169 (2022)
- Wang, X., Sun, S., Kampen, E., Chu, Q.: Quadrotor fault tolerant incremental sliding mode control driven by sliding mode disturbance observers. *Aerosp. Sci. Technol.* **87**, 417–430 (2019)
- Li, S., Wang, Y., Tan, J., Zheng, Y.: Adaptive RBFNNs/integral sliding mode control for a quadrotor aircraft. *Neurocomputing* **216**, 126–134 (2016)
- Li, B., Gong, W., Yang, Y., Xiao, B., Ran, D.: Appointed fixed time observer-based sliding mode control for a quadrotor UAV under external disturbances. *IEEE Trans. Aerosp. Electron. Syst.* **58**(1), 290–303 (2022)
- Mofid, O., Mobayen, S.: Adaptive sliding mode control for finite-time stability of quad-rotor UAVs with parametric uncertainties. *ISA Trans.* **72**, 1–14 (2018)
- Shao, X., Sun, G., Yao, W., Liu, J., Wu, L.: Adaptive sliding mode control for quadrotor UAVs with input saturation. *IEEE/ASME Trans. Mechatron.* **27**(3), 1498–1509 (2022)
- Tang, P., Zhang, F., Ye, J., Lin, D.: An integral TSMC-based adaptive fault-tolerant control for quadrotor with external disturbances and parametric uncertainties. *Aerosp. Sci. Technol.* **109**, 106415 (2021)
- Nekoukar, V., Dehkordi, N.M.: Robust path tracking of a quadrotor using adaptive fuzzy terminal sliding mode control. *Control. Eng. Pract.* **110**, 104763 (2021)
- Xiong, J., Zhang, G.: Global fast dynamic terminal sliding mode control for a quadrotor UAV. *ISA Trans.* **66**, 233–240 (2017)
- Wang, F., Gao, H., Wang, K., Zhao, C., Zong, Q., Hua, C.: Disturbance observer-based finite-time control design for a quadrotor UAV with external disturbance. *IEEE Trans. Aerosp. Electron. Syst.* **57**(2), 834–847 (2021)
- Liang, S., Meng, W., Lin, Z., Shao, K., Zheng, J., Li, H., Lu, R.: Adaptive attitude control of a quadrotor using fast non-singular terminal sliding mode. *IEEE Trans. Ind. Electron.* **69**(2), 1597–1607 (2022)
- Das, A., Lewis, F., Subbarao, K.: Backstepping approach for controlling a quadrotor using Lagrange form dynamics. *J. Intell. Robot. Syst.* **56**, 127–151 (2009)
- Wang, R., Liu, J.: Trajectory tracking control of a 6-DOF quadrotor UAV with input saturation via backstepping. *J. Franklin Inst.* **355**, 3288–3309 (2018)
- Ma, D., Xia, Y., Shen, G., Jia, Z., Li, T.: Flatness-based adaptive sliding mode tracking control for a quadrotor with disturbances. *J. Franklin Inst.* **355**, 6300–6322 (2018)
- Derrouaoui, S.H., Bouzid, Y., Guiatni, M.: PSO based optimal gain scheduling backstepping flight controller design for a transformable quadrotor. *J. Intell. Robot. Syst.* **102**(67), 1–25 (2021)
- Li, C., Zhang, Y., Li, P.: Full control of a quadrotor using parameter-scheduled backstepping method: implementation

- and experimental tests. *Nonlinear Dyn.* **89**, 1259–1278 (2017)
23. Cui, G., Yang, W., Yu, J., Li, Z., Tao, C.: Fixed-time prescribed performance adaptive trajectory tracking control for a QUAV. *IEEE Trans. Circuits Syst. II Express Brief* **69**(2), 494–498 (2022)
 24. Liu, K., Wang, R.: Antisaturation command filtered backstepping control-based disturbance rejection for a quadrotor UAV. *IEEE Trans. Circuits Syst. II Express Brief* **68**(12), 3577–3581 (2021)
 25. Shao, X., Liu, J., Wang, H.: Robust back-stepping output feedback trajectory tracking for quadrotors via extended state observer and sigmoid tracking differentiator. *Mech. Syst. Signal Process.* **104**, 631–647 (2018)
 26. Lu, H., Liu, C., Coombes, M., Guo, L., Chen, W.: Online optimisation-based backstepping control design with application to quadrotor. *IET Control Theory Appl.* **10**(14), 1601–1611 (2016)
 27. Basri, M.A.M.: Trajectory tracking control of autonomous quadrotor helicopter using robust neural adaptive backstepping approach. *J. Aerosp. Eng.* **31**(2), 04017091 (2018)
 28. Xie, W., Cabecinhas, D., Cunha, R., Silvestre, C.: Adaptive backstepping control of a quadcopter with uncertain vehicle mass, moment of inertia, and disturbances. *IEEE Trans. Ind. Electron.* **69**(1), 549–559 (2022)
 29. Ahmed, N., Raza, A., Shah, S., Khan, K.: Robust composite-disturbance observer based flight control of quadrotor attitude. *J. Intell. Robot. Syst.* **103**(11), 1–18 (2021)
 30. Jia, Z., Yu, J., Mei, Y., Chen, Y., Shen, Y., Ai, X.: Integral backstepping sliding mode control for quadrotor helicopter under external uncertain disturbances. *Aerosp. Sci. Technol.* **68**, 299–307 (2017)
 31. Wang, H., Li, N., Wang, Y., Su, B.: Backstepping sliding mode trajectory tracking via extended state observer for quadrotors with wind disturbance. *Int. J. Control Autom. Syst.* **19**(10), 3273–3284 (2021)
 32. Zhao, J., Ding, X., Jiang, B., Jiang, G., Xie, F.: A novel control strategy for quadrotors with variable mass and external disturbance. *Int. J. Robust Nonlinear Control* **31**(17), 8605–8631 (2021)
 33. Elikar, K., Grouni, S., Tadjine, M., Zhang, W.: Quadcopter nonsingular finite-time adaptive robust saturated command-filtered control system under the presence of uncertainties and input saturation. *Nonlinear Dyn.* **104**(2), 1363–1387 (2021)
 34. Castillo, A., Sanz, R., Garcia, P., Qiu, W., Wang, H., Xu, C.: Disturbance observer-based quadrotor attitude tracking control for aggressive maneuvers. *Control. Eng. Pract.* **82**, 14–23 (2019)
 35. Xiao, B., Yin, S.: A new disturbance attenuation control scheme for quadrotor unmanned aerial vehicles. *IEEE Trans. Ind. Inf.* **13**(6), 2922–2932 (2017)
 36. Bisheban, M., Lee, T.: Geometric adaptive control with neural networks for a quadrotor in wind fields. *IEEE Trans. Control Syst. Technol.* **29**(4), 1533–1548 (2021)
 37. Khodamipour, G., Khorashadizadeh, S., Farshad, M.: Observer-based adaptive control of robot manipulators using reinforcement learning and the Fourier series expansion. *Trans. Inst. Meas. Control.* **43**(10), 2307–2320 (2021)
 38. Asignacion, A., Suzuki, S., Noda, R., Nakata, T., Liu, H.: Frequency-based wind gust estimation for quadrotors using a nonlinear disturbance observer. *IEEE Robot. Autom. Lett.* **7**(4), 9224–9231 (2022)
 39. Tian, B., Cui, J., Lu, H., Zuo, Z., Zong, Q.: Adaptive finite-time attitude tracking of quadrotors with experiments and comparisons. *IEEE Trans. Ind. Electron.* **66**(12), 9428–9438 (2019)
 40. Slotine, J.E., Li, W.: *Applied Nonlinear Control*. China Machine Press, Beijing (2004)
 41. Horn, R.A., Johnson, C.R.: *Matrix Analysis*. Cambridge University Press, Cambridge (2013)
 42. Miklos, L., Vera, T.: *Real Analysis: Foundations and Functions of One Variable*. Springer, Berlin (2015)
 43. Masjed-Jamei, M.: A functional generalization of the Cauchy–Schwarz inequality and some subclasses. *Appl. Math. Lett.* **22**(9), 1335–1339 (2009)
 44. Nagesh, I., Edwards, C.: Adaptive finite-time attitude tracking of quadrotors with experiments and comparisons. *Automatica* **50**(3), 984–988 (2014)
 45. Gonzalez, T., Moreno, J.A., Fridman, L.: Variable gain super-twisting sliding mode control. *IEEE Trans. Autom. Control* **57**(8), 2100–2105 (2012)
 46. Wang, X., Shirinzadeh, B., Ang, M.H.J.: Nonlinear double-integral observer and application to quadrotor aircraft. *IEEE Trans. Ind. Electron.* **62**(2), 1189–1200 (2015)
 47. Izadbakhsh, A., Khorashadizadeh, S.: Polynomial-based robust adaptive impedance control of electrically driven robots. *Robotica* **39**(7), 1181–1201 (2021)
 48. Xu, Y., Shmaliy, Y.S., Shen, T., Chen, D., Sun, M., Zhang, Y.: INS/UWB-based quadrotor localization under colored measurement noise. *IEEE Sens. J.* **21**(5), 6384–6392 (2021)

Publisher's Note Springer Nature remains neutral with regard to jurisdictional claims in published maps and institutional affiliations.

Springer Nature or its licensor (e.g. a society or other partner) holds exclusive rights to this article under a publishing agreement with the author(s) or other rightsholder(s); author self-archiving of the accepted manuscript version of this article is solely governed by the terms of such publishing agreement and applicable law.